

Safeguarding Navigation in Automated Shipping Through 3D Modelling and Reconstruction of Maritime Objects Using Segmented LiDAR Point Clouds

D. Yacoub, C. Petersen & M. Steidel
German Aerospace Center (DLR), Oldenburg, Germany

ABSTRACT: The accurate perception of the environment of vessels is essential for the development of automated maritime systems and remote operation, as it is important to ensure a safe navigation in narrow fairways and in harbor areas. LiDAR (Light Detection and Ranging) scanners are widely used in object detection applications, as they produce dense 3D point clouds. However, due to their line-of-sight limitations, only partial views of objects are recorded, making a full shape reconstruction necessary for safe navigation and situational awareness. This paper presents a method to reconstruct full object dimensions from incomplete LiDAR measurements. We introduce an automated selection algorithm that chooses the most suitable model from segmented point clouds based on geometric characteristics, aiming to reconstruct full object shapes. To improve modeling accuracy for navigation, we evaluate three advanced models compared to the Box Model: Cylinder Model, L-Shape Box Fitting, and Elliptic Cylinder Fitting. The reconstruction accuracy is quantified using the root mean squared error (RMSE) by comparing the fitted models against ground-truth point clouds compiled from multi-view scans. Furthermore, we compare the error of our proposed selection method to the box model, providing insight into its advantages and limitations for maritime object modeling. Field tests with representative maritime objects from two harbor locations are presented. The results show that the choice of reconstruction method plays a key role in how accurately maritime objects can be modeled. Simple shapes such as buoys, pontoons and piles are well represented by basic models, whereas complex or irregular structures require more flexible reconstruction methods, such as Triangle Mesh. Adapting the modeling technique to object geometry reduces manual and computational effort while supporting reliable navigation and autonomous operation.

1 INTRODUCTION

The current development of the maritime domain is showing applications of new automated systems as well as the application of Maritime Remote Operation, even going as far as autonomous or remotely operated vessels already being in use [1]. These initiatives are intensified due to various technological developments, but also induced by the shortage of skilled labor in the maritime industry [2]. For the remote operation of vessels, it is especially important that the remote operator is able to handle typical tasks in navigation,

such as avoiding collisions with other vessels or with the maritime infrastructure. This can be hindered when the remote operator is not able to assess the environment of the vessel due to no sufficient data being available, which is even more crucial in narrow harbor areas or fairways. Misjudging the environment and obstacles in harbor areas can lead to costly incidents [3], potentially putting other participants and the environment at danger. Using highly automated systems without having information on the surrounding environment is challenging, as it is harder to safely navigate near these structures. This is also

crucial in applications in which the vessel needs to fully rely on the information from its sensors. As an example, Figure 1 is showing a challenging situation in the Jarßum Harbor in Emden. The research vessel is approaching an area with a crane, which presents several obstacles, notably the base of the crane, marked in red. These maritime objects should be represented precisely, also considering their shape and dimension. While it is possible to view the surrounding environment by looking at the camera picture, it is challenging to fully understand the dimensions of obstacles as well as to perceive the depth information. This is crucial information that is needed to safeguard navigation in automated and remote-controlled applications.



Figure 1. Crane in the Jarßum Harbor in Emden, as seen from the research vessel. The crane foundation on the left side is marked in red.

Already used for sensing the environment and detecting these objects are technologies such as radars, cameras or LiDAR scanners [4], which are installed on vessels. For example, LiDAR scanners can help to provide the needed depth information as described above. As unprocessed LiDAR data is complex, a reliable solution is needed that can provide dimensions or features of single objects, effectively supporting remote operators and automated systems. LiDAR is well-suited to object detection because it can measure distances very precisely and capture a dense 3D image. Unlike a passive camera, it is not dependent on ambient light conditions, making it a reliable choice for sensing the environment. However, raw LiDAR point clouds are unstructured and noisy. Therefore, it is difficult to use it for navigation purposes in this unprocessed state and it has to be processed and enhanced in order to be used for information of the vessel's surrounding. For navigation, further approaches exist to map the maritime environment in harbors, such as in [5], aiming to improve conventional Electronic Navigational Charts (ENC) by adding 3D information from LiDAR scans, although mentioning the need for retrieving the full shape of the detected object from a single LiDAR scan.

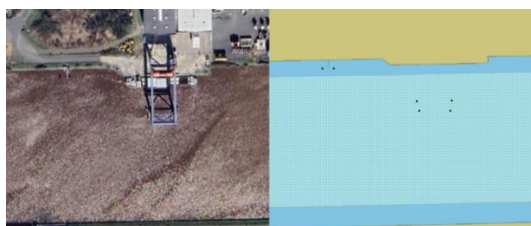


Figure 2. Comparison between satellite image and ENC for the Jarßum Harbor in Emden. (Sources: Imagery ©2024 AeroWest, Airbus, CNES / Airbus, Maxar Technologies, Map data ©2024 GeoBasis-DE/BKG (©2009), Google (left), Professional+ chart data from Lloyd's Register/i4Insight in a ChartServer solution from ChartWorld (right))

As can be seen in Figure 2, details in an ENC can vary significantly compared to the actual shapes of objects present. The crane in the satellite image is not represented properly in the ENC, and relying on this chart as a remote operator can be burdensome. Retrieving the full shape of detected objects presents a challenge due to factors such as varying object geometries and incomplete point clouds, when objects are only captured from one direction at a time. This questions how LiDAR measurements in maritime environments can be reconstructed to improve awareness on the vessel's surrounding.

Regarding the reconstruction of incomplete LiDAR measurements, most previous work uses either complete scans or simple box models for the reconstruction of LiDAR point clouds. In practice, especially in harbor environments, LiDAR scans are often incomplete, and depending only on the box models can lead to incorrect safety distances or unnecessarily long routes during navigation. While LiDAR nowadays is commonly used in the maritime domain, incomplete measurements can be challenging for navigation as already described. In these applications, dimensions of objects and the depth information are crucial. To address this problem, we introduce an algorithm that automatically selects the most suitable reconstruction method based on the geometry of segmented LiDAR data. We investigate three alternative modeling methods, namely Cylinder Model, L-Shape Box Fitting and Elliptic Cylinder Fitting compared to the Box Model, that are better suited to maritime objects with rectangular, circular or elliptical shapes in their XY projection. As no single model is equally effective in all cases, our algorithm determines the most suitable model. This approach reduces manual effort and computation time while improving reconstruction accuracy. We validate our approach using various maritime objects recorded in the Jarßum Harbor in Emden and the Oldenburg Harbor, using root mean square error (RMSE) as evaluation metric. The results demonstrate how adaptive model selection can improve the reliability and safety of LiDAR point clouds for remote and autonomous vessel operation. While this study focuses on regular-shaped objects, more complex maritime structures may require alternative reconstruction methods such as Triangle Mesh approaches, which are discussed later in this paper.

2 RELATED WORK

Object reconstruction using LiDAR has been studied in various fields, including autonomous driving [6, 7] and autonomous maritime applications [9]. Working with LiDAR point clouds often is dealing with incomplete or irregular data, making it necessary to segment the point cloud into clusters to improve the quality of 3D reconstructions.

Automotive applications focus on object detection and tracking as in [6], or approximating object shapes and modeling obstacles [8] in order to improve the safety of driver assistance systems. In the maritime domain, applications include the sensor-supported modeling and tracking of vessels and floating structures as in [9], to be used in route planning and collision avoidance.

In these applications for the related literature described above, several geometric models are applied in order to estimate shapes of the objects. As an example, the Box Model is a method in which objects are approximated using rectangular volumes, making it a standard approach for object modelling. Krämer [6] uses box boundary surfaces for automatic detection from LiDAR and approximates these surfaces by adapting algorithms from [10]. This approach offers a method that can also be used for detecting maritime objects. Similarly, Ali et al. [7] extend the YOLO3D loss function to include yaw angle, 3D box center, and height for real-time oriented 3D bounding box detection from LiDAR point clouds. The YOLO3D is a variant of the popular YOLO algorithm, specifically designed for 3D object detection, while traditional YOLO models detect objects in 2D images.

For objects with cylindrical or round geometries, the Cylindrical Model offers a more accurate reconstruction than the Box Model. The study by Nurunnabiet al. [11] proposes robust cylinder fitting methods using point cloud data, which can be adapted for detecting cylindrical maritime objects, even when LiDAR data is noisy or incomplete.

Additionally, the L-Shape fitting method is suitable for modelling objects with L-shaped structures. In related work, Zhang et al. [10] describe L-Shape fitting as an optimization problem for vehicle detection using laser scanners, while Shen et al. [8] present an efficient algorithm that segments point clouds and fits them with perpendicular lines. This technique can be adapted for maritime objects with L-shaped or edged features. In addition to L-Shape fitting, Lin et al. [9] employ Elliptic Fitting specifically for maritime objects, using LiDAR point clouds to model them as bounding boxes or elliptic cylinders, thereby offering a different approach for varied maritime geometries.

The models discussed work well for objects with regular shapes, more complex maritime structures often require different reconstruction methods. One alternative solution in such cases is Triangle Mesh reconstruction. Researchers such as Carlberg et al. [12], Gopi and Krishnan [13] and Marton et al. [14] have developed algorithms that generate triangular meshes from disorganised point clouds, with a focus on mesh initialisation, growth and refinement. Krämer [6] later adapted these methods for automated driving. However, these ideas could also be applied in a maritime context to more accurately capture complex maritime objects.

While these approaches provide valuable insights into the applications of various geometric models to maritime objects, a comprehensive evaluation of how to effectively apply these models to maritime structures remains incomplete. Further, a method that can supply dimensions and depth information of maritime objects to be used in navigation applications is needed. This highlights the need for selecting and adapting suitable models that can efficiently and robustly reconstruct maritime objects from LiDAR data, as information on the dimensions of maritime objects or obstacles as well as the depth information is necessary to have. Geometric models are differing in their complexity, depending on the desired application and object type. The following section therefore presents our algorithm for selecting the most

appropriate reconstruction method based on the geometry of the maritime object, while considering different geometric models and their accuracy of representation.

3 CONCEPT

3.1 Reconstruction of Maritime Objects using LiDAR point clouds

As LiDAR scans from a single position only allow the front side of objects to be captured, a reconstruction of incomplete LiDAR point clouds is needed in order to map current maritime environment conditions and to enable a 3D perception of this environment. We propose to fuse LiDAR and GNSS (Global Navigation Satellite System) data in order to achieve a geo-localization of the LiDAR scans. The complex geo-referenced LiDAR point clouds will be processed with different geometry-based methods in order to reconstruct shapes and dimension of these objects. The overall process is showcased in Figure 3, displaying all needed steps in order to reconstruct objects from the LiDAR point clouds.

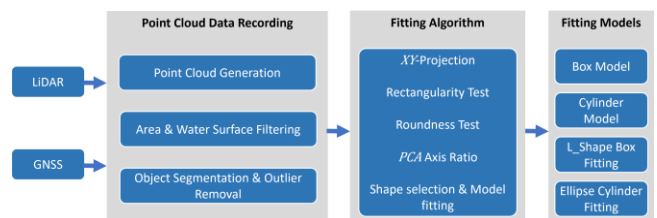


Figure 3. Processing steps for LiDAR point cloud reconstruction

LiDAR and GNSS data are the inputs needed for the following processing steps. The step Point Cloud Data Recording handles the processing of the LiDAR point cloud, resulting in several point clouds with containing single maritime objects. Here, the LiDAR and GNSS data is fused, effectively leading to the point cloud having a precise geo-position. Then, the point clouds have to be filtered. This is done by selecting the area of interest, so that only maritime objects are included in the point cloud. Afterwards, all points below the water surface are removed, as only objects above the water surface can be reliably detected with the LiDAR scanner and water reflections will hinder the reconstruction process. Then, all objects are segmented from the LiDAR point cloud and outliers are removed to reduce noise. The next step Fitting Algorithm (chapter 3.3) estimates shapes for the maritime objects and applies models according to the step Fitting Models (chapter 3.2). These processing steps are applied and evaluated in chapter 4.

3.2 Geometric Models for the Reconstruction of Maritime Objects from LiDAR Data

In maritime environments, accurate reconstruction of object surfaces from LiDAR data depends on the geometric characteristics of the object. Accordingly, different surface fitting models can be applied. The following models represent commonly used approaches for approximating the shapes of maritime objects based on incomplete segmented LiDAR point

clouds. As these models are important for our proposed algorithm, the models will be described first.

3.2.1 Box Model

The Box Surface Model has become the standard geometric model for objects in automated driving [6]. This model approximates the object's surface with a box-shaped structure. The box surface

$$S_{Box} = (c, \psi, W, L, H)$$

is represented by the dimensions of the Box W, L and H , which are calculated as follows:

$$W = x_{\max} - x_{\min}, \quad L = y_{\max} - y_{\min}, \quad H = z_{\max} - z_{\min}$$

where $x_{\max}, x_{\min}, y_{\max}, y_{\min}, z_{\max}, z_{\min}$ are the minimum and maximum coordinates of the segmented LiDAR points along each axis.

The center position c of the box is defined as:

$$c = (W/2, L/2, H/2)$$

Finally, the yaw angle ψ , which represents the object's rotation around the vertical Z-axis, is estimated by:

$$\psi = \text{atan2}(L, W)$$

To determine an initial estimate for the Box Model parameters from segmented LiDAR data, the box fitting algorithm described by Zhang et al. [10] is used. This method involves uniformly choosing the space of possible box orientations (ψ) within the range $[0, \pi)$, taking advantage of the Box Model's symmetry. For each candidate angle, a closeness score C is computed to evaluate the fit:

$$C = \sum_{i=1}^N \frac{1}{\max(d_i, d_{\min})}$$

where d_i is the distance from the i -th scan point to the closest edge of the bounding box and d_{\min} is the lower cut-off distance threshold that reduces the influence of points close to the object's edge. The bounding box with the highest closeness score provides an approximate initial guess for the object's position, orientation, width, length, and height.

The box surface model provides a fast and simple fit suitable for all object types, but it offers limited shape accuracy. Therefore, in cases where maritime objects have regular geometric forms such as cylinders, elliptical cylinders or even cuboids, alternative modeling methods including precise cuboid models should be selected to ensure higher accuracy.

3.2.2 Cylinder Model

The Cylinder Model is important for many applications of 3D point clouds, for example in autonomous navigation [11]. The model is defined by:

$$S_{Cylinder} = (c, r, H)$$

where $c \in \mathbb{R}^3$ is the center of the cylinder, r is the radius and H is the height along the Z-axis.

To compute the radius r , the 3D segmented point cloud is projected onto the XY-plane. The minimum enclosing circle is then determined using Welzl's algorithm [15]. This method returns the circle center (x_c, y_c) and the radius r :

$$r = \min_{\text{EnclosingCircle}} (P_{xy})$$

The height H is calculated as:

$$H = z_{\max} - z_{\min}$$

Finally, the 3D center c is computed as:

$$c = \left(x_c, y_c, \frac{H}{2} \right)$$

The Cylinder Model is well suited for objects with cylindrical geometries such as poles or pipes [11], although provides lower accuracy for box-shaped, angular, or elliptic cylindrical structures.

3.2.3 Shape-Fitting Method

L-Shape Box Fitting and Elliptic Cylinder Shape Fitting are commonly used to approximate shapes [9]. Both methods start with a point set $S \in \mathbb{R}^{n \times 2}$, defined by x - and y -coordinates. The goal is to represent the object's geometry angular in L-Shape Fitting and curved in Elliptic Fitting. In both methods, the height of the Box or Elliptic Cylinder is determined by the vertical distance between the highest and lowest z -values.

1. L-Shape Box Fitting Method

An L-shaped rectangle is fitted, as described in [9], to a 2D point cluster $S = \{(x_i, y_i) | i=1, 2, \dots, n\}$ by dividing it into two disjoint subsets P and Q , such that $P \cup Q = S$, $P \cap Q = \emptyset$. Each subset is associated with one of two perpendicular lines:

$$l_1 : x_i \cos \theta + y_i \sin \theta = c_1, \quad l_2 : -x_i \sin \theta + y_i \cos \theta = c_2$$

The optimal parameters θ, c_1, c_2 are found by minimizing the sum of squared distances from the points to their respective lines. The solution to this optimization problem yields the parameters of the two straight lines that best approximate the edges of the L-shaped object. The rectangle's corner points are then determined by identifying the farthest associated points along each fitted line, following the method described by [9]. Two diagonal corner points P_1 and P_2 are identified, one with the minimum, the other with the maximum x or y value. The third corner is the point farthest from the diagonal line $\overline{P_1 P_2}$, completing the L-shape rectangle. The fitted 2D L-shape rectangle is extended along the Z-axis to create a three-dimensional L-Shaped Box Fitting.

2. Elliptic Cylinder Fitting

An ellipse in 2D can be described parametrically as follows:

$$x(t) = x_c + a \cos(t) \cos(\theta) - b \sin(t) \sin(\theta)$$

$$y(t) = y_c + a \cos(t) \sin(\theta) + b \sin(t) \cos(\theta),$$

with $t \in [0, 2\pi]$

Here, a denotes the semi-major axis, b the semi-minor axis, and θ the rotation angle of the ellipse with respect to the X-axis. (x_c, y_c) represents the center of the ellipse in the XY-plane. This formulation results from applying a 2D rotation and translation to the standard ellipse equation.

When fitting an ellipse to a point cloud, especially when outliers exist, the RANSAC (Random Sample Consensus) algorithm [16] is employed.

1. Sampling: Random subsets of points in the XY-plane are selected.
2. Model Estimation: Each subset is used to estimate an ellipse (center, axes, angle).
3. Model Evaluation: The remaining points within a threshold are inliers; others are outliers.
4. Optimization: The ellipse with the most inliers is chosen.

The 2D ellipse is then extended along the Z-axis into an elliptical cylinder, where the height is determined by the lowest and highest points in the z-values.

3.3 Fitting Method Selection Algorithm Based on Object Geometry

Since the characteristics of the described models can affect their accuracy when applied to point clouds, it is essential to select an appropriate geometric model for each object. This is particularly important because it is often difficult to determine the exact shape of an object based only on its point cloud representation. Manual selection of geometric models entails the risk of inaccurate reconstruction, particularly when only partial point clouds are available. Therefore, an automated approach is required to identify the most suitable geometric model for the reconstruction of maritime objects.

In this section, we address these challenges by proposing an automated algorithm that determines whether an object is best represented by an L-Shape Box, a Cylinder Model, or an Elliptical Cylinder, based on the geometry of its 2D projection from the point cloud. These three geometric models were chosen because they accurately represent the most common shapes found in maritime environments, while also ensuring that the object's height can be derived consistently from LiDAR observations. The proposed algorithm operates through the following steps:

3.3.1 Point Cloud Projection:

As a first step, the segmented 3D point cloud is projected onto the XY-plane. This projection reduces the dimensionality of the data and simplifies the analysis of the object's ground projection. However, since LiDAR measurements in maritime environments are often incomplete, the projected shape is not always clearly defined. Therefore, the ground projection must be further examined to determine whether it is best fitted as rectangular, circular, or elliptical.

3.3.2 Rectangularity Test:

To identify rectangular shapes, the convex hull of the projected points is first analysed. A line is estimated using the RANSAC algorithm [16, 17], which estimates model parameters by repeatedly selecting random subsets of points and evaluating the model that best fits the largest consensus set of inliers. After this step, the inliers of the first line are removed, and a second line is estimated using RANSAC on the remaining points. If both lines are nearly orthogonal and each is supported by a sufficient number of inliers, the object is classified as rectangular. In this case, the selected geometric model is the L-Shape Box.

3.3.3 Roundness Test (Circle vs. Ellipse)

If the rectangularity test fails and as we are only considering maritime objects with regular shapes, the object is considered to be round. Two parallel RANSAC procedures are applied:

- RANSAC_circle: tests for circularity using small random point subsets.
- RANSAC_ellipse: tests for ellipticity in the same manner.

Both follow the Efficient-RANSAC strategy [18], which robustly detects shapes by repeatedly sampling small random subsets and selecting the model supported by the greatest number of inliers. Once the best candidate is identified, the corresponding inliers are refitted using least-squares methods for improved accuracy:

- For circles: classical least-squares circle solvers [17], which minimize the distance of the points to an ideal circular model.
- For ellipses: direct least-squares ellipse solvers [19], which formulate the problem as a generalized eigenvalue problem to estimate ellipse parameters.
- To further distinguish between circular and elliptical shapes, the following additional criterion is used.

3.3.4 The Axis Ratio (Eigenvalue Ratio):

As an additional criterion, the Principal Component Analysis (PCA) is applied to the 2D shape obtained from the roundness test [20]. PCA rotates the point cloud so that one axis corresponds to the direction of greatest variation in the points, while the other axis corresponds to the least variation. The eigenvalues λ_1 and λ_2 representing the variance along the principal directions. The Axis Ratio is defined as:

$$R = \frac{\lambda_1}{\lambda_2}, \quad \lambda_1 \geq \lambda_2$$

- If $R \approx 1$, the shape is close to a circle, and the selected geometric model is the Cylinder Model.
- If $R > 1$, the shape is elongated, representing an ellipse, and the corresponding model is the Elliptical Cylinder Fitting.

The proposed algorithm is specifically designed for regular geometries, i.e., objects that can be approximated by rectangular, circular, or elliptical projections. In cases where objects consist of irregular or complex geometries, the method becomes less suitable, and a more generalized approach, such as triangulated mesh reconstruction or convex hull

approximation, is required. To test and validate the proposed reconstruction methods, field experiments were conducted at different locations with various maritime objects. The following section in chapter 4 describes the acquired data and evaluation.

4 APPLICATION & EVALUATION

This chapter focuses on applying the described process model on real world data. For this, point cloud data from field tests are used. Maritime objects are segmented from these LiDAR scans and the Fitting Method Selection Algorithm is applied on this data. The accuracy of the results is evaluated by comparing single LiDAR scans to a combined LiDAR ground truth.

4.1 Field tests

In order to apply the shape fitting methods, sufficient LiDAR data from the real world is needed that represents relevant maritime objects. For this, field tests are conducted in three different test locations, containing different maritime objects of interest. The specifications of these test locations are displayed in Table 1. Used in this measuring campaign is a high-resolution LiDAR scanner stationed on the quay walls to record comprehensive data from multiple angles of each test location. A vessel-based sensor setup is not used at this stage, as the focus on these maritime objects allows a high-resolution scanner to fully scan these objects from the quay walls in a controlled environment. These LiDAR scans are georeferenced by using GNSS data, with the accuracy being increased by correctional measurements of Real-Time Kinematic-GPS. By georeferencing each single LiDAR scan, the foundation is set to combine the single scans of a location in order to obtain a full representation of the specific location. This setup allows for the creation of a ground truth dataset through combination of the collected data, so that objects in each location are fully captured from all angles.

Table 1. Field test locations

Test location	Location type	Scan positions
Emden	Seaport	7
Oldenburg (South)	Waterway	4
Oldenburg (North)	Inland Port	5

In the Jarßum Harbor in Emden, the most relevant object is the crane, which is also visible in the satellite image in Figure 2. Further, a vessel is available in the data, which was present at the time of recording LiDAR data in the harbor area. For the two locations in Oldenburg (Figure 4), the southern area includes data of a bridge and buoys, while the northern area includes different mooring facilities. Overall, the recordings result to about 18.4 GB of LiDAR and GNSS data from these three locations.



Figure 4. Aerial image of both test locations in Oldenburg (Imagery ©2024 Airbus, GeoBasis-DE/BKG, Maxar Technologies, Map data ©2025, Google)

4.2 Evaluation data

For further usage, maritime objects of interest are segmented from the LiDAR point clouds. First, the area of interest is filtered. As a next step, single objects are segmented from the area of interest. For the LiDAR data from the test locations a manual segmentation is conducted. The LiDAR point clouds for separated maritime objects are filtered in order to remove outliers, aiming to further reduce noise. This same procedure is applied to multiple objects captured in the field tests. With the data from these point clouds for maritime objects it is now possible to apply the fitting algorithm in order to find fitting models and evaluate the accuracy of the selected models. Used for the evaluation purposes of the Fitting Method Selection Algorithm are maritime objects from these LiDAR scans, namely the buoy (scanned in Oldenburg) as well as the vessel and the two parts of the base of the crane (scanned in Emden).

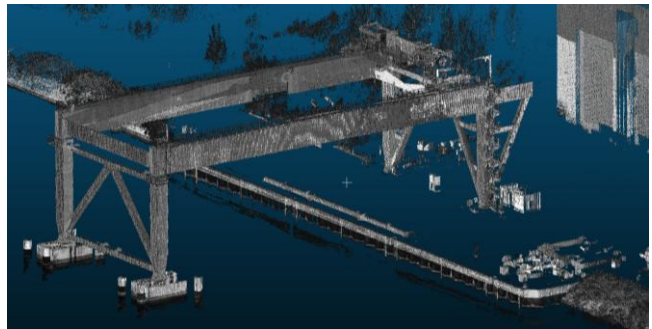


Figure 5. Unfiltered LiDAR point cloud of the crane in the Jarßum Harbor in Emden.

Figure 5 is showing a combined point cloud of multiple LiDAR scans for the crane in the Jarßum Harbor in Emden. The data is unfiltered and therefore including several objects nearby. The data in Figure 6 has been filtered and only the base of the crane is visible. In this case, only a single LiDAR scan is shown.

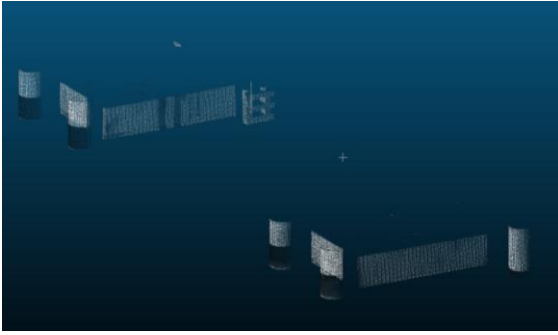


Figure 6. Area of interest for a single scan for the crane in the Jarßum Harbor in Emden.

4.3 Validation on Maritime Objects

We validated the Fitting Method Selection Algorithm based on object geometry in field tests implemented in Oldenburg and Emden. For the evaluation of maritime objects, four different object types that met the selection criteria were selected, as already described in chapter 4.2. Tables 2 to 5 show these objects, with the buoy being scanned in Oldenburg and the other objects scanned in Emden. Tables 2 and 4 show the foundation of the crane in the Jarßum Harbor in Emden, which can reconstruct the full foundation of the crane when the results for the reconstructed models are combined. For the crane base (see Table 2), running two-line RANSAC on the convex hull points yields two nearly orthogonal directions supported by many points, the rectangularity test is therefore passed and the suggested 3D model is an L-shaped box.

For the buoy, crane pile, and vessel (see Tables 3–5), no pair of perpendicular edges is detected, so their cross-sections are treated as round. We then perform a model competition (circle vs. ellipse) using Efficient RANSAC, followed by least-squares refitting of the selected curve. For the buoy and crane pile, the PCA axis ratio $R \approx 1$, and the circle is selected as the best fit, the recommended 3D model is a Cylinder. For the vessel, $R > 1$; indicates elongation, therefore the ellipse is chosen, yielding an Elliptical Cylinder.

Table 2. From left to right: (1) photo of the crane base; (2) its 3D point cloud; (3) XY-plane projection with a bounding; (4) resulting suggested model (L-shape box).


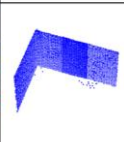
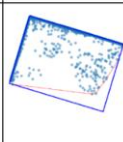
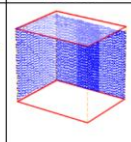
Object – Crane Base	Point Cloud	Projection Form	Suggested Model
			

Table 3. From left to right: (1) photo of the buoy; (2) its 3D point cloud; (3) XY-plane projection with a bounding and the eigenvalues; (4) resulting suggested model (Cylinder).


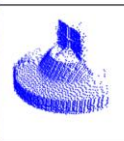
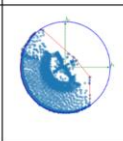
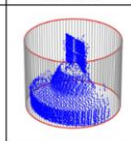
Object – Buoy	Point Cloud	Projection Form	Suggested Model
			

Table 4. From left to right: (1) photo of the crane pile; (2) its 3D point cloud; (3) XY-plane projection with a bounding and the eigenvalues; (4) resulting suggested model (Cylinder).


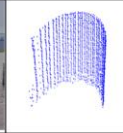
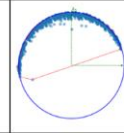
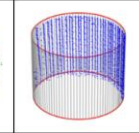


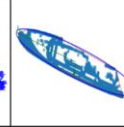
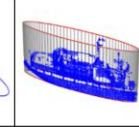
Object – Crane Pile	Point Cloud	Projection Form	Suggested Model
			

Table 5. From left to right: (1) photo of the crane base; (2) its 3D point cloud; (3) XY-plane projection with a bounding and the eigenvalues; (4) resulting suggested model (Elliptical Cylinder).

Object – Vessel	Point Cloud	Projection Form	Suggested Model
			

In summary, results for the selected objects show that the proposed algorithm is suited for segmented LiDAR point clouds of maritime objects, where cross-sections can be represented by simple shapes such as rectangles, circles, or ellipses, and the appropriate 3D model can be assigned. However, the algorithm is not intended to handle very complex objects in a single step. In such cases, the object should first be divided into simpler parts, and the fitting method can then be applied to each part. For highly irregular or detailed structures, alternative approaches such as triangle mesh reconstruction are required. Additionally, the processing time is strongly influenced by the complexity of the object and the number of points in the LiDAR dataset. Simpler shapes with fewer points, like buoys or piles, can be reconstructed much faster since they require fewer optimization steps and simpler calculations. In contrast, large or complex structures, such as vessels or cranes with detailed components, need more time for segmentation, filtering, and model fitting because of their more detailed surfaces and higher point densities.

4.4 Evaluation of maritime objects from field test


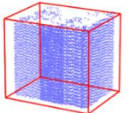
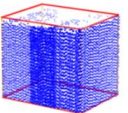
Now that the shape of the maritime objects has been determined from the point cloud data as described in the Fitting Method Selection Algorithm, the accuracy of these fits can get evaluated. The geometric accuracy of reconstructed maritime objects from incomplete LiDAR point clouds is evaluated using the Root Mean Square Error (RMSE). In this context, RMSE quantifies how closely the reconstructed model matches the actual geometry of the object. By scanning an object from all sides and using these scans as ground truth, it is possible to accurately determine the geometric deviation between the reconstructed model and the original object. The distance from each point on the original point cloud to the surface of the fitted model is calculated using the following formula:

$$RMSE = \sqrt{\frac{1}{N} \sum_{i=1}^N d_i^2}$$

Here, d_i represents the shortest distance from the i -th point in the ground truth point cloud to the surface of the fitted model, and N denotes the total number of points in the ground truth cloud. A lower RMSE value denotes a more accurate reconstruction.

For evaluation, the four object types introduced above are used. The model chosen by the selection algorithm is compared against the Box Surface Model, the model with the lower RMSE is considered more accurate.

Table 6. Evaluation results for crane base object

Object – Crane Base	Box Model	Selected Model
		
-	RMSE (Box) = 1.65	RMSE (L-Shape Box) = 0.70

For the crane-base, the algorithm selected L-Shape Box fitting, reducing RMSE to 0.70 m compared with 1.65 m for the Box Model.

Table 7. Evaluation results for buoy object


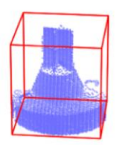
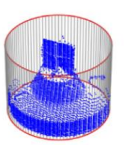

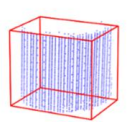
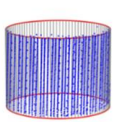
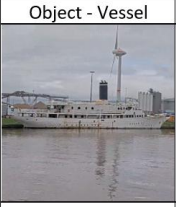
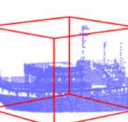
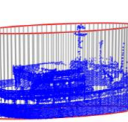
Object - Buoy	Box Model	Selected Model
		
$R = 1.02$	RMSE (Box) = 0.57	RMSE (Cylinder) = 0.43

Table 8. Evaluation results for crane pile object

Object – Crane Pile	Box Model	Selected Model
		
$R = 1.2$	RMSE (Box) = 0.84	RMSE (Cylinder) = 0.76

For the buoy and the crane-pile ($R \approx 1$), the algorithm proposed a cylinder model, yielding lower RMSEs than the Box Model 0.43 m versus 0.57 m for the buoy and 0.76 m versus 0.84 m for the crane pile. This improved performance shows that the accuracy of the geometric representation is increased, as the algorithm determines a better fit for a cylindrical shape.

Table 9. Evaluation results for vessel object

Object - Vessel	Box Model	Selected Model
		
$R = 38.44$	RMSE (Box) = 14.78	RMSE (Elliptic Cylinder) = 5.88

For the vessel ($R > 1$), an elliptic-cylinder fit achieved an RMSE of 5.88 compared with 14.78 for the Box Model.

The results show that the choice of an appropriate reconstruction model depends on the detected shape and therefore used model by the Fitting Method Selection Algorithm that has been validated by the RMSE score. An adaptive model choice offers a clear advantage over a Box Model, as it provides a more

accurate geometric representation of regular maritime objects and ensures an essential requirement for robust applications in navigation and remote operation.

5 TECHNOLOGICAL CHALLENGES

This chapter will discuss identified challenges for the reliable reconstruction of maritime objects captured by LiDAR scanners. One major challenge is how complex object shapes can be reconstructed in the future, aiming at precisely representing their true shapes.

5.1 Reconstruction of complex and irregular shapes

When maritime objects with complex shapes need to be reconstructed, the geometric models described in chapter 3.2 can be insufficient for these objects. The Triangle Mesh Method has been studied as an approach for reconstructing 3D surfaces from LiDAR point clouds, particularly in the automotive domain [6]. However, its application in maritime contexts has received little attention. This section discusses the 3D Delaunay Mesh Method for reconstructing maritime objects, especially irregular and complex structures, from LiDAR point clouds. A 3D Delaunay Triangulation connects points in a 3D space to form non-overlapping tetrahedra that represent the surface of the object. In practice, the Delaunay property alone is not sufficient, and it is necessary to impose quality constraints governing the shape, size, and angles of the elements. This process is called Delaunay mesh refinement, as introduced by [21]. The Delaunay Refinement ensures that the points are connected in such a way that no point is inside the circumsphere (in 3D) of any of the tetrahedra. In 2D, this would be the circumcircle of the triangles. Further, the Delaunay refinement also aims to improve the shape quality of the mesh elements by maximizing the minimum angle of the tetrahedra triangles (or triangles in 2D). These criteria ensure that the resulting Delaunay triangulation is well-shaped and connected, which is all important for accurately modelling objects in 3D. Figure 7 shows an example for two maritime objects.

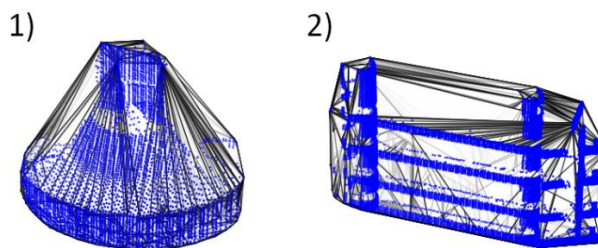


Figure 7. Two examples of Triangle Mesh applications on maritime objects. Left (1): A simple object where applying a mesh adds little value. Right (2): A complex object where meshing enables a more detailed and precise reconstruction.

This approach is particularly useful for irregularly shaped maritime objects, when a more precise reconstruction is needed that cannot be achieved with the models described above. However, these detailed models may require more computational resources. For regular structures, the Triangle Mesh method may not be necessary, and simpler geometric models may be more practical and efficient.

5.2 Selection of technologies

Challenging as well is the selection of technologies in order to capture the maritime environment and to process LiDAR point clouds for the reconstruction. Used for the evaluation of this work was a high-resolution LiDAR scanner stationed on the quay wall, while mobile LiDAR scanners on vessels are likely to have a lower resolution of the resulting point clouds. Here, it is important to consider how far away the scanned maritime objects are, as closer objects will be captured in a higher resolution. Further, how many points of an object exist in the point cloud will have an impact on the processing speed for the LiDAR reconstruction, as more points describe a more computationally demanding problem.

6 CONCLUSION AND FUTURE WORK

In this study, several methods were evaluated for reconstructing 3D models of maritime objects based on incomplete LiDAR point cloud data, with the goal of supporting reliable object representation in autonomous systems and maritime navigation. For reconstruction, LiDAR data was used from field trials in two locations. Results from evaluating the Fitting Method Selection Algorithm showed that the reconstruction method decides how accurately maritime objects are modeled and that our proposed method is able to detect the shapes of the geometries in the LiDAR point clouds. The comparison of Box-, Cylinder-Model, L-Shape Box- and Elliptic Cylinder-Fitting, as well as the outlook towards Triangle Mesh approaches showed that each method has specific advantages depending on the object's geometry and complexity. The results confirm the importance of choosing a modelling method that aligns reconstruction accuracy with the geometric characteristics of the object. Future work will aim to extend the modelling methods to a wider range of maritime object classes. This includes improving the representation of complex structures, such as modelling a crane as a single object rather than as multiple components. Triangle Mesh Methods will be applied for modelling irregular shapes and fully reconstructing of detailed objects. In the future, these advanced modelling techniques can be integrated into maritime systems. Their deployment in navigational applications and for Remote Operation is expected to enhance Situation Awareness and aid in safeguarding automated systems. Further future use cases include route planning and collision avoidance applications in both autonomous and remotely operated maritime environments.

REFERENCES

- [1] Kongsberg, The first electric autonomous ship ever. [Online]. Available: <https://protect.kongsberg.com/kongsberg---the-first-electric-autonomous-ship-ever/> (accessed: Jul. 14 2025).
- [2] BIMCO and International Chamber of Shipping, Seafarer Workforce Report - The global supply and demand for seafarers in 2021. [Online]. Available: <https://www.bimco.org/products/publications/titles/seafarer-workforce-report/> (accessed: Jul. 14 2025).
- [3] Marine Insight News Network, "Real Life Incident: Passenger Ship Strikes Pier Causing Damage Worth \$2.1 Million," *Marine Insight*, 06 Oct., 2023. <https://www.marineinsight.com/case-studies/real-life-incident-docking-knock/> (accessed: Jul. 14 2025).
- [4] S. Thombre et al., "Sensors and AI Techniques for Situational Awareness in Autonomous Ships: A Review," *IEEE Trans. Intell. Transport. Syst.*, vol. 23, no. 1, pp. 64–83, 2022, doi: 10.1109/TITS.2020.3023957.
- [5] C. Petersen, F. Pieper, A. Bokern, and M. Steidel, "Enhancing Situation Awareness in Highly Automated Shipping using High-Resolution Electronic Navigational Charts," in *Proceedings of the MARESEC 2024*.
- [6] S. Krämer, "LiDAR-Based Object Tracking and Shape Estimation," Dissertation from the KIT Faculty of Mechanical Engineering of the Karlsruhe Institute of Technology, 2020. [Online]. Available: <https://publikationen.bibliothek.kit.edu/1000130358>
- [7] W. Ali, S. Abdelkarim, M. Zahran, M. Zidan, and A. El Sallab, "YOLO3D: End-to-end real-time 3D Oriented Object Bounding Box Detection from LiDAR Point Cloud," arXiv:1808.02350v1, 2018.
- [8] X. Shen, S. Pendleton, and M. H. Ang, "Efficient L-shape fitting of laser scanner data for vehicle pose estimation," *IEEE 7th International Conference on Cybernetics and Intelligent Systems (CIS) and IEEE Conference on Robotics, Automation and Mechatronics*, 2015.
- [9] J. LIN, G. CAMPA, C.-E. Framing, J.-J. Gehrt, R. Zweigel, and D. Abel, "Adaptive Shape Fitting for Lidar object Detection and Tracking in Maritime Applications," *International Journal of Transport Development and Integration*, 2021.
- [10] X. Zhang, W. Xu, C. Dong, and J. M. Dolan, "Efficient L-Shape Fitting for Vehicle Detection Using Laser Scanners," *IEEE Intelligent Vehicles Symposium (IV 2017)*. Redondo Beach, CA, USA,, 2017.
- [11] A. Nurunnabi, Y. Sadahiro, R. Lindenbergh, and D. Belton, "Robust cylinder fitting in laser scanning point cloud data," *Measurement Volume 138*, vol. 2019, pp. 632–651, 2019.
- [12] M. Carlberg, J. Andrews, P. Gao, and Zakhor Avideh, "Fast Surface Reconstruction and Segmentation with Ground-Based and Airborne LIDAR Range Data," Tech. rep. Berkeley, USA: UC Berkeley, 2008.
- [13] M. Gopi and S. Krishnan, "A Fast and Efficient Projection-Based Approach for Surface Reconstruction," *XV Brazilian Symposium on Computer Graphics and Image Processing*. Fortaleza, Brazil, 2002.
- [14] Marton, Zoltan, Csaba, Rusu, Radu, Bogdan, and Beetz Michael, "On Fast Surface Reconstruction Methods for Large and Noisy Point Clouds," *IEEE International Conference on Robotics and Automation (ICRA 2009)*. Kobe, Japan, 2009, pp. 2829–2834, 2009.
- [15] E. Welzl, "Smallest enclosing disks (balls and ellipsoids)," *New Results and New Trends in Computer Science*, vol. 1991, pp. 359–370, 1991.
- [16] Shenghui Xu, "RANSAC based three points algorithm for ellipse fitting of spherical object's projection," arXiv:1503.07460, 2015.
- [17] N. Chernov and C. Lesort, "Least squares fitting of circles and lines," 2003.
- [18] R. Schnabel, R. Wahl, and R. Klein, "Efficient RANSAC for Point - Cloud Shape Detection," *Computer Graphics Forum*, vol. 26, no. 2, pp. 214 – 226, 2007, doi: 10.1111/j.1467-8659.2007.01016.x.
- [19] A. Fitzgibbon, M. Pilu, and R. B. Fisher, "Direct least square fitting of ellipses," *IEEE Trans. Pattern Anal. Machine Intell.*, vol. 21, no. 5, pp. 476–480, 1999, doi: 10.1109/34.765658.
- [20] I. T. Jolliffe and J. Cadima, "Principal component analysis: a review and recent developments," *Philosophical transactions. Series A, Mathematical, physical, and engineering sciences*, vol. 374, no. 2065, p. 20150202, 2016, doi: 10.1098/rsta.2015.0202.

- [21] J. R. Shewchuk, "Delaunay refinement algorithms for triangular mesh generation," *Computational Geometry* 22, vol. 2002, pp. 21–74, 2002.